



HAL
open science

Innovative Approach to Use Air Bearings in Cubesat Ground Tests

Irina Gavrilovich, Sébastien Krut, Marc Gouttefarde, François Pierrot,
Laurent Dusseau

► **To cite this version:**

Irina Gavrilovich, Sébastien Krut, Marc Gouttefarde, François Pierrot, Laurent Dusseau. Innovative Approach to Use Air Bearings in Cubesat Ground Tests. CubeSat Workshop, ESA, CNES, May 2016, La Valette, Malta. hal-01348039

HAL Id: hal-01348039

<https://hal.science/hal-01348039>

Submitted on 22 Jul 2016

HAL is a multi-disciplinary open access archive for the deposit and dissemination of scientific research documents, whether they are published or not. The documents may come from teaching and research institutions in France or abroad, or from public or private research centers.

L'archive ouverte pluridisciplinaire **HAL**, est destinée au dépôt et à la diffusion de documents scientifiques de niveau recherche, publiés ou non, émanant des établissements d'enseignement et de recherche français ou étrangers, des laboratoires publics ou privés.

INNOVATIVE APPROACH TO USE AIR BEARINGS IN CUBESAT GROUND TESTS

Irina Gavrilovich⁽¹⁾, Sébastien Krut⁽¹⁾, Marc Gouttefarde⁽¹⁾, François Pierrot⁽¹⁾, Laurent Dusseau⁽²⁾

⁽¹⁾ *Laboratory of Informatics, Robotics and Microelectronics, University of Montpellier - CNRS, 161 rue Ada, 34095 Montpellier, France, +33 467 41 85 85*

{irina.gavrilovich, sebastien.krut, marc.gouttefarde, francois.pierrot}@lirmm.fr

⁽²⁾ *Montpellier-Nîmes University Space Center, University of Montpellier, CC 06-011 Campus St Priest, Bat. 6, 860 rue St Priest, 34090 Montpellier, France, +33 467 14 38 25, laurent.dusseau@iut-nimes.fr*

ABSTRACT

In the fast-growing society of CubeSat developers, the necessity of CubeSat ground tests is apparent. One of the more complex and discussed system-level tests is the Attitude Determination and Control System (ADCS) examination. It requires motions of the CubeSat and environment conditions close to space. Most of the ADCS testbeds involve an air bearing as one of the main component of a rotating table since it allows reducing the friction between the moving CubeSat and fixed elements. However, such rotating tables have common drawbacks. Notably, they allow CubeSat rotations only in a limited range of angles, usually within $\pm 45^\circ$. In this paper, an innovative approach to use air bearings, which allows circumventing this limitation, is discussed. The proposed testbed involves 4 air bearings instead of only one. The air bearings are placed so that their effective surfaces lie on a sphere. This (virtual) sphere is large enough to place a CubeSat inside, while its influence on the dynamic parameters of the CubeSat is minimal. Nevertheless, some issues should be tackled to ensure the feasibility of such an air bearing testbed. In the proposed design, the concentricity of the air bearing active elements and the floating spherical elements might be perturbed and thus affect the lift force. In addition, the total lift force of the air bearing sphere highly depends on the angular attitude of the sphere. This paper presents results of the study of the air bearing sphere behavior and the progress of the work which has been previously introduced at the 4S Symposium in 2014.

1 INTRODUCTION

Every CubeSat developer meets the necessity of pre-launch ground tests and deals with them in his own way, depending on several factors: The complexity of the satellite subsystems and planned mission, the number of space qualified components, experience in space technologies and the time left before launch. However, when the mission and the CubeSat are complicated, safety and the omission of some tests are critical issues [1]. One of the more complex and discussed system-level tests is the Attitude Determination and Control System (ADCS) examination. It requires motions of the CubeSat and environment conditions close to space. To this end, the testing facilities are usually equipped with sun and star sky simulators, a Helmholtz cage, a rotating table, and monitoring tools. The rotating table is the most problematic element of the ADCS testing facilities. It is supposed to mitigate all influences on the satellite that disturb its free motion during tests.

Most of the ADCS testbeds involve an air bearing as one of the main component of the rotating table since it allows reducing the friction between the moving CubeSat and the testbed fixed elements. There are different types of air bearing platforms employed for these purposes and the

most widely used type is a tabletop system [2]. It includes a spherical air bearing and a plate placed on top of a floating hemisphere. Because of the geometrical constraints of such a design, rotational freedom is limited to $\pm 45^\circ$ from the horizon, while having full freedom of spin [6]-[10]. These restrictions affect the efficiency of the testbed and the reliability of the ADCS ground tests.

An alternative concept of a testbed with 4 air bearings instead of one has been proposed in [3]. The air bearings are placed on one spherical surface so that their effective surfaces form a virtual sphere large enough to include a CubeSat with attached floating spherical elements (passive elements of the air bearing). To ensure that the 4 passive elements always face the air bearing active elements (i.e. parts through which the air blows) a robotic arm will be used. It allows moving the active elements in space by tracking the attitude of the CubeSat. This design has obvious advantages including potentially unconstrained CubeSat rotations during ADCS tests, minimized disturbing influence of the rotating table on the CubeSat, and minimized friction. Such a use of air bearings is different from the usual one and the behavior of the air bearing sphere shall be studied to ensure the feasibility of the system.

The main air bearing characteristic is the lift force. Besides the size and geometry of the air bearing, it also depends on fly height of the payload, i.e. a distance between the air bearing and the payload at equilibrium state. In the system described above, the fly height varies greatly while the air bearing sphere rotates. At the same time, normal air bearing behavior is restricted by the geometry of the sphere. That means, the fly heights and lift forces of the air bearings are coupled and they depend on the sphere orientation. Together with fly heights, the CubeSat position inside the virtual sphere varies. In order to minimize the influence of this motion on the test results, fluctuations of the CubeSat inside the air bearing sphere shall be studied. To this end, a study of the air bearing assembly in terms of lift forces and fly heights is presented in this paper. Additionally, this study helps to ensure that the air bearing active and passive elements do not collide whatever the orientation of the sphere is.

2 TESTBED PROTOTYPE

The enlargement of the range of the operation angles of the testbed has major impact upon its efficiency. The concept of the air bearing sphere originates from the idea to place the satellites in a hollow sphere levitating on a single air bearing. Improving this basic idea, the 4 air bearing sphere eliminates an obvious drawback, namely, large mass of the whole sphere compared to the CubeSat, and hence, a notable change of the CubeSat dynamic parameters. The advantages of the concept of the testbed proposed in this work are detailed in previous publications of the authors [3], [4].

For the experimental verification of the air bearing sphere testbed, a prototype has been designed. It has a structure similar to the design in [3], but operability of the prototype has several limitations. The testbed prototype consists of the following parts: (i) the CubeSat mock-up with air bearing passive elements attached to it (the Inner Sphere); (ii) the air bearing active elements hold by the rigid frame (the Outer Sphere) and (iii) the robotic arm (Fig. 1). The Inner Sphere is free to move and follow the trajectory pre-defined for the CubeSat test, while the robotic arm moves the Outer Sphere to keep the active and passive elements of the air bearings aligned. The relative orientation of the active and passive elements is measured by means of distance sensors and used in real time to generate the robot motion. While the correction of the Outer Sphere orientation is realized expeditiously, minimal mismatch between the active and passive elements orientation might take place. For the 40 mm air bearings, this mismatch shall be no more than 3° according to the preliminary tests.

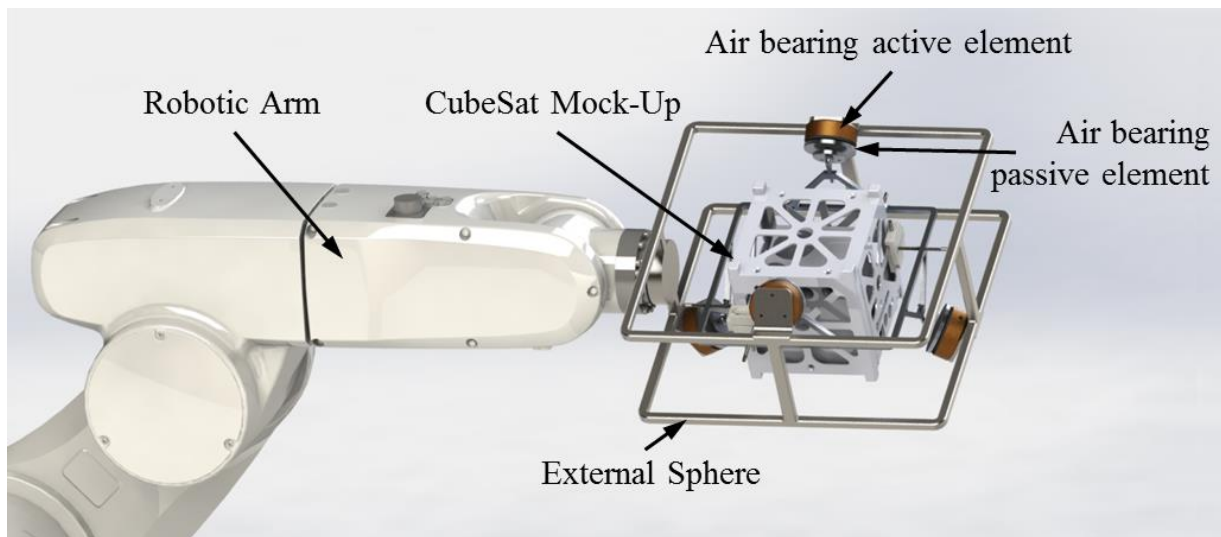


Figure 1. The testbed prototype overview

3 AIR BEARING PROPERTIES

Air bearings are widely used in different engineering applications, such as measuring and precision machines, space-oriented facilities, and other clean room, high speed, and precise applications. Air bearings allow zero static and minimized dynamic friction, zero wear, silent and smooth operation, high speed and high acceleration. In satellite testbeds, air bearings are chosen primarily because of reduced friction that allows free rotation of the structure containing the satellite and leads to realistic simulation of the satellite dynamics in space [11]. For the testbed studied in this paper, spherical air bearings are chosen. Their geometry consists of a cylindrical (diameter 40mm) portion of a 105mm radius sphere (Fig. 1).

One of the concerns about air bearings is their stiffness. They provide high dynamic stiffness, which meanwhile depends on the lift force. The theoretical plot of the lift force as function of the payload fly height for the air bearing used in the testbed is shown in Fig. 2. It has been identified on the statistical data of air bearings and the local stiffness value taken from the data sheet of the chosen air bearing [5]. The slope of the curve in Fig. 2 is not linear and as the air film gets thinner the stiffness gets higher. Pressure and surface area both affect stiffness proportionately.

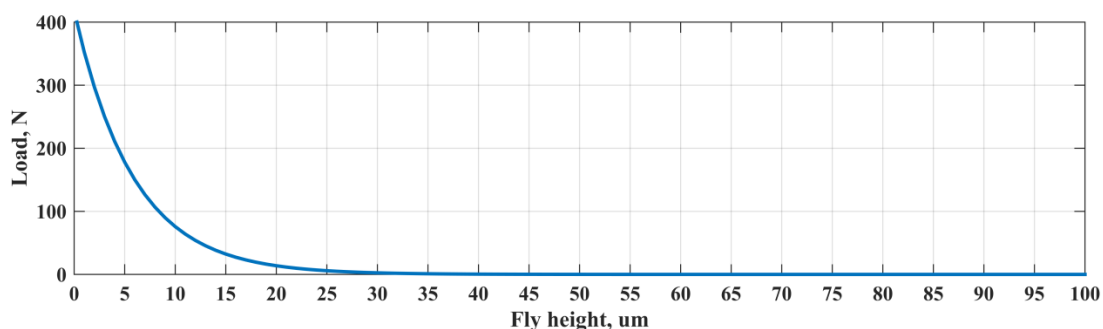


Figure 2. Load versus fly height curve. The local slope represents the local stiffness

4 BEHAVIOR OF THE AIR BEARING SPHERES

4.1 Geometry and assumptions

According to the design of the testbed, the air bearings have some geometrical restrictions. The Inner Sphere is placed inside the Outer Sphere such that the sphere formed by the passive elements of the air bearings is smaller than the one formed by the active elements. For normal operation of the test bench, the Inner Sphere can move inside the Outer Sphere, but the minimum clearance between them shall be always $>0\mu\text{m}$, in other words, the Spheres shall not collide. If the air bearing assembly would be a complete sphere, the Inner Sphere would fall a little onto the Outer Sphere, till equilibrium for the lift force that counteract the Inner Sphere weight is found. This vertical deviation would be constant, independent from the angular positions of the Spheres. However, the Spheres are composed of 4 separated air bearings, as described above, and the total lift force of the Outer Sphere onto the Inner Sphere depends on their orientation. The study of the relative Inner Sphere - Outer Sphere deviation, together with the corresponding bearing lift forces through a range of angular positions is presented below.

The geometry of the air bearing assembly made with 4 spherical air bearings evenly spread in space can be modelled as shown in Fig. 3. The air bearings active elements are mounted on the Outer Sphere by means of spherical joints, thus the linear displacements are constrained while the angular displacements are possible. Due to this mounting the active air bearing elements can be represented by the force pointed to the geometry centre (GC) of the Outer Sphere.

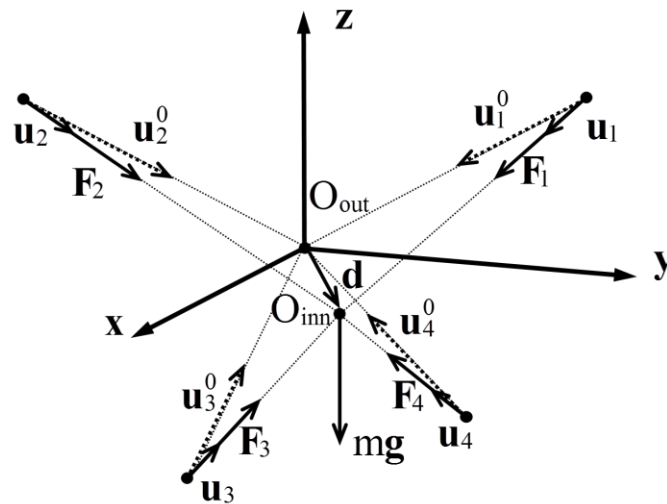


Figure 3. Free body diagram of the Inner Sphere

In Fig. 3, \mathbf{F}_i is the lift force of an air bearing, \mathbf{u}_i is the unit vector directing \mathbf{F}_i (it starts at the centre of an air bearing and is pointed towards the centre of the Inner Sphere O_{inn} , assuming the lift force is normal to the air bearing passive element), and \mathbf{u}_i^0 is the unit vector pointed towards the centre of the Outer Sphere O_{out} . Vector \mathbf{d} stands for the displacement vector of O_{inn} with respect to O_{out} . Vector mg corresponds to the weight of the Inner Sphere.

In this model, the following assumptions are made:

1. The Inner Sphere is considered to be a rigid body with its GC coincident with its centre of mass (CoM) at point O_{inn} .
2. Vectors \mathbf{u}_i and \mathbf{u}_i^0 are collinear. Indeed, displacement \mathbf{d} is few orders of magnitude smaller

than the radius of the Spheres, that causes negligibly small misalignment of vectors \mathbf{u}_i and \mathbf{u}_i^0 .

3. As a consequence of Assumption 2, if at any orientation, the Inner and Outer Spheres are not concentric, this does not affect the direction of the forces generated by the air bearings and they are assumed to be pointed towards O_{out} . Practically in such a case, the radius vector of the force changes its orientation, because it is pointed towards O_{inn} and it might affect the dynamics of the Spheres. Possible change of the force vectors shall be considered in further studies.
4. The tangent component of the air bearing force is assumed to be negligible compared to the normal component. Experimental data might bring us to change this assumption later.

4.2 Study of the spheres motion

Considering the system quasi-static, Euler's law of motion can be written:

$$\sum_{i=1..4} \mathbf{F}_i + m\mathbf{g} = 0 \quad (1)$$

As it was highlighted in Fig. 2, the lift force of the air bearing is a function of the fly height. The shape of the curve in Fig. 2 is modelled by the exponential function $f(x) = 0.843^x$ based on an identification process. Thus, the lift force is estimated by:

$$\mathbf{F}_i = F_0 \cdot 0.843^{h_i-5} \mathbf{u}_i \quad (2)$$

where the nominal lift force F_0 is the force at 5 μm fly height (default value from the air bearing data sheet). For the chosen air bearing $F_0 = 178\text{N}$; h_i is a fly height along the direction \mathbf{u}_i in micron:

$$h_i = h_a + \mathbf{d} \cdot \mathbf{u}_i \quad (3)$$

where h_a is a sphere gap found as $h_a = r_{out} - r_{inn}$; r_{out} and r_{inn} are radii of the Outer and Inner Spheres (μm) respectively.

Substituting Eqs. 2 – 3 into Eq. 1, the following system of equations is obtained:

$$F_0 \cdot 0.843^{h_a-5} (0.843^{\mathbf{d} \cdot \mathbf{u}_1} \mathbf{u}_1 + 0.843^{\mathbf{d} \cdot \mathbf{u}_2} \mathbf{u}_2 + 0.843^{\mathbf{d} \cdot \mathbf{u}_3} \mathbf{u}_3 + 0.843^{\mathbf{d} \cdot \mathbf{u}_4} \mathbf{u}_4) + m\mathbf{g} = 0 \quad (4)$$

Considering $\mathbf{u}_i(\alpha, \beta, \gamma)$ as a function of three rotational angles α, β, γ , and \mathbf{d} as an unknown vector, the system in Eq. 4 has 3 equations and 3 unknowns. However, it contains non-linear (exponential) dependencies that justify the usage of a numerical solver.

4.3 Spring in the system

Since the clearance between the Spheres is of the order of microns, the assembling and setting of the Spheres shall be done very accurate, that might be difficult to implement. In order to minimize the requirements of setting the Spheres, a spring is used in the mounting of one of the four air bearing active elements on the Outer Sphere. A prismatic joint is used so that this active element can only translate radially.

Considering only the Inner Sphere, the free body diagram is similar to that in Fig. 3. The Euler's law of motion for the Inner Sphere is similar to Eq. 1. The forces provided by rigidly connected air

bearing active elements \mathbf{F}_i are assigned according to Eq. 2. Force \mathbf{F}_4 , associated with the air bearing with a spring, is given by the following equation:

$$\mathbf{F}_4 = F_0 \cdot 0.043^{h_a + \mathbf{d} \cdot \mathbf{u}_i - h_{sp} - 5} \mathbf{u}_4 \quad (5)$$

where h_{sp} is spring deformation (μm).

For the air bearing active element, attached through the spring to the Outer Sphere, the free body diagram is shown in Fig. 4.

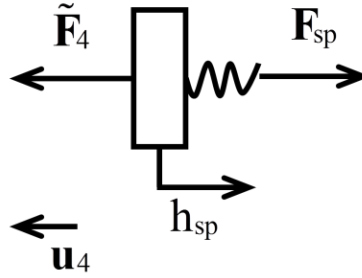


Figure 4. Free body diagram of the air bearing active element with a spring

Forces $\tilde{\mathbf{F}}_4$ and \mathbf{F}_4 have the same amplitude and opposite directions. The spring is modelled as follows:

$$F_{sp} = F_{sp}^0 + kh_{sp} \quad (6)$$

where F_{sp}^0 is the force that the spring provides at its initial deformation (corresponding to the case where the air bearing active element is on the sphere with the other active elements); k is the spring stiffness coefficient; k is equal to 0 when a constant force spring is chosen.

Combining Eqs. 4 – 6, the following system of equations is obtained:

$$\begin{cases} F_0 \cdot 0.843^{h_a - 5} (0.843^{\mathbf{d} \cdot \mathbf{u}_1} \mathbf{u}_1 + 0.843^{\mathbf{d} \cdot \mathbf{u}_2} \mathbf{u}_2 + 0.843^{\mathbf{d} \cdot \mathbf{u}_3} \mathbf{u}_3 + 0.843^{\mathbf{d} \cdot \mathbf{u}_4 - h_{sp}} \mathbf{u}_4) + m\mathbf{g} = 0 \\ F_{sp} = F_{sp}^0 + kh_{sp} \end{cases} \quad (7)$$

Here, the forces can be decoupled from the displacement \mathbf{d} , because only 3 forces are left independent. Then Eq. 7 is easier to solve with respect to \mathbf{F}_i :

$$F_1 \mathbf{u}_1 + F_2 \mathbf{u}_2 + F_3 \mathbf{u}_3 + F_{sp} \mathbf{u}_4 + m\mathbf{g} = 0 \quad (8)$$

System Eq. 8 contains 3 unknown forces F_1, F_2, F_3 and 3 linear equations, which uniquely define these forces.

5 RESULTS AND DISCUSSIONS

Eqs. 4 and 8 are used to simulate the behavior of the air bearing assembly. Results in Fig. 5 and 7 show lift forces, fly heights and coordinates of the Inner Sphere CoM as functions of the Spheres orientation, for the rigidly connected air bearings and the system with a spring, respectively. Influence of the various sphere gaps on the motion of the Inner Sphere CoM is shown in Fig. 6 and in Fig. 8.

The following parameters are used in simulations:

Radius of the Inner Sphere	105mm
Mass of the Inner Sphere	3kg
Air bearing force at 5 μ m fly height	178N
Spring force at initial deformations	50N
Spring stiffness coefficient	0N/ μ m (constant force spring)
Motion	Rotation with constant velocity 1 $^\circ$ /sec around Y

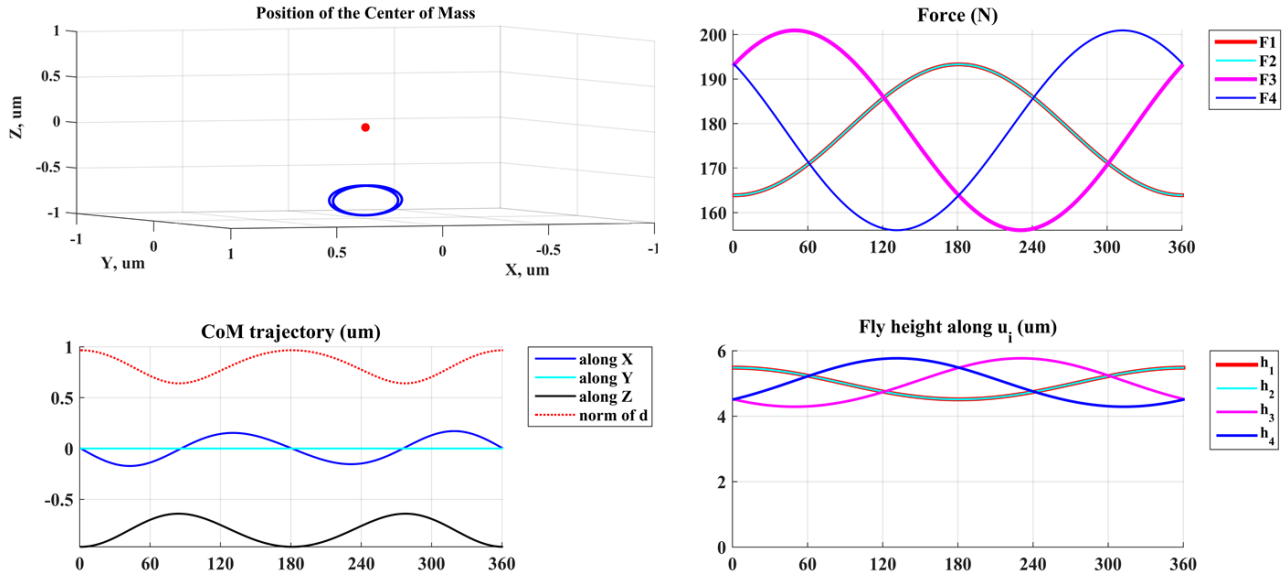


Figure 5. Left - Motion of the CoM of the Inner Sphere; right - force diagram at different angular orientations and fly heights along the axis of each air bearing. Sphere gap 5 μ m

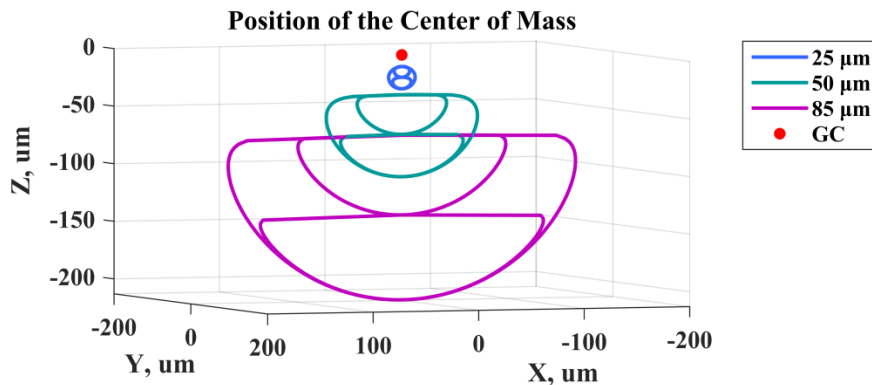


Figure 6. Motion of the CoM of the Inner Sphere with different sphere gaps: 25, 50 and 85 μ m

When all air bearings are rigidly connected, their fly heights (and, consequently, lift forces as it follows from Eq. 2) are coupled and depend on the sphere gap. Then, Eq. 3 shows that the Inner Sphere CoM displacement \mathbf{d} is a function of the fly height and the sphere gap. As result, the position of the Inner Sphere CoM in the Outer Sphere largely fluctuates when the spheres rotate and this fluctuation is getting worst with larger sphere gap. This statement is illustrated in Fig. 6 for CoM trajectories with 3 different sphere gaps.

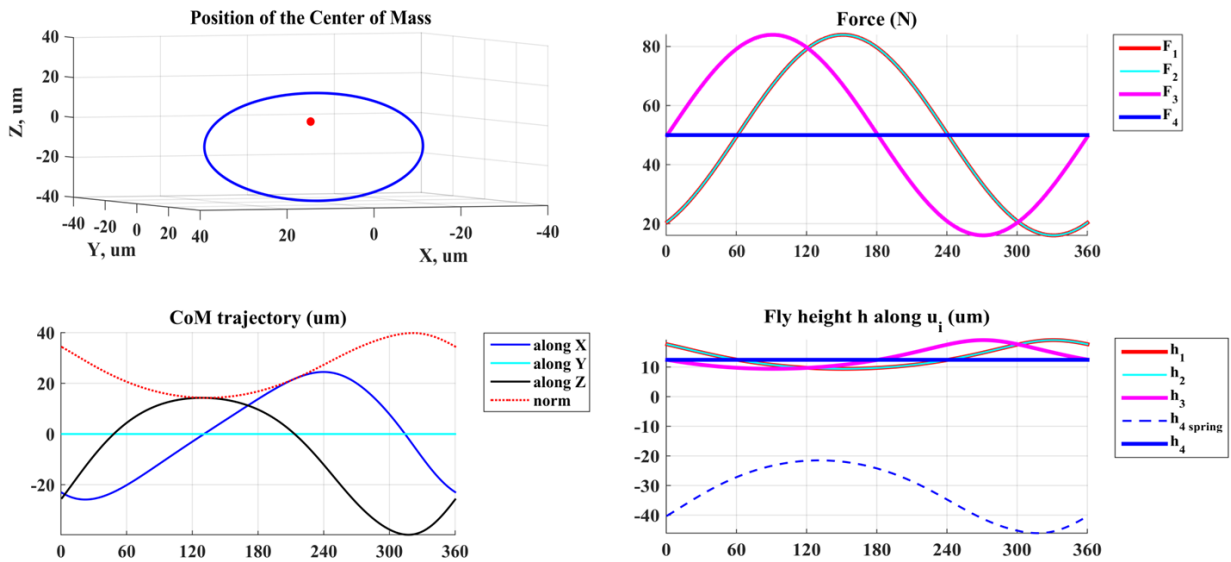


Figure 7. Left - Motion of the CoM of the Inner Sphere; right - force diagram at different angular orientations and fly heights along the axis of each air bearing. Sphere gap 5 μm

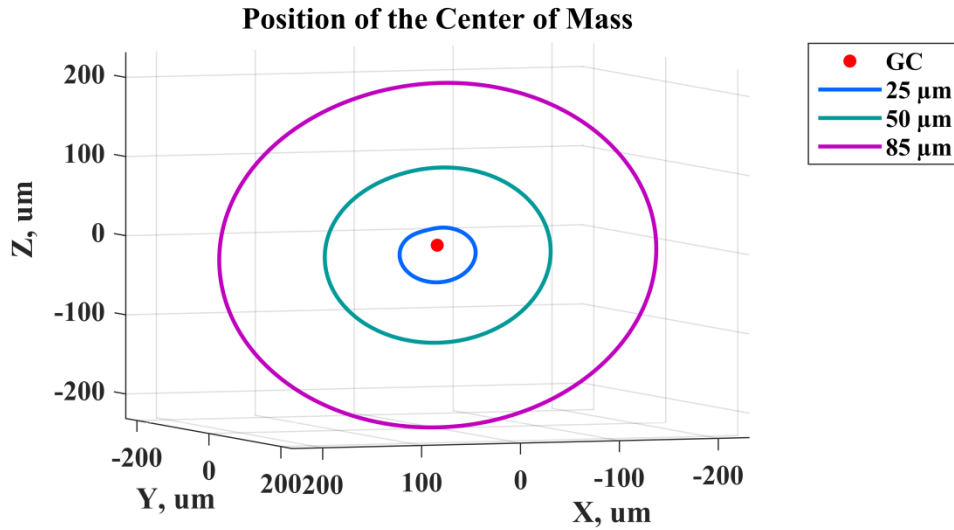


Figure 8. Motion of the CoM of the Inner Sphere with different sphere gaps: 25, 50 and 85 μm

Analysing Eqs. 7 and 8 for the system with a spring, it is easy to see that the system is not over constrained anymore and it has only three variable forces to define three coordinates. Then lift forces are functions $F_{i=1,2,3} = f(F_{sp}, m, \alpha, \beta, \gamma)$ and independent of the other parameters. It means that the spring force distinctively defines lift forces of three fixed air bearings and these forces stay the same with any sphere gap.

The fly height is defined as follows:

$$h_{i=1..4} = \log_{0.843} (F_i/F_0) \quad (9)$$

As (9) is a logarithmic function, for the system with a spring, the fly heights can be uniquely

defined for given parameters of the system as $h_{i=1..4} = f(F_0, F_{sp}, m, \alpha, \beta, \gamma)$ and do not depend on the sphere gap any more.

The displacement \mathbf{d} is coupled with the sphere gap and the fly height as given by Eq. 3, such that $d = f(h_a, F_0, F_{sp}, m, \alpha, \beta, \gamma)$. Coupling with the sphere gap is linear and considering the character of the fly height function, it is easy to see that the Inner Sphere CoM does not move with respect to the Outer Sphere, but together with it (Fig. 8). This is the desired behavior for the air bearing sphere application on the testbed.

6 CONCLUSION

In this paper the recent progress of the developing the air bearing testbed for CubeSats is presented. This testbed concept is based on use of the air bearing sphere (4 air bearings are located so that their effective surfaces form a sphere) which potentially expands the operability range of the testbed and improves its efficiency. This principle of the air bearing application is unusual and requires an additional study. Understanding of the air bearing sphere behavior is important for the realization of the testbed with such technology. Study of the sphere shows, that the CubeSat obtains some motion within the testbed due to the alternate lift force of air bearings. In order to avoid these undesired fluctuations of the CubeSat inside the testbed, a spring is proposed to be used to preload one of the air bearings. With a spring, system is not over constrained anymore, so use of a spring makes the relative motion of CubeSat smoother and helps to decrease requirements to the assembling of the testbed.

7 ACKNOWLEDGMENTS

This research work was funded by The Van Allen Foundation of the University of Montpellier.

8 REFERENCES

- [1] Swartwout M., *The First One Hundred CubeSats: A Statistical Look*, JoSS, Vol.2, No.2, pp. 213-233, 2013.
- [2] Schwartz J.L., Peck M.A. and Hall Ch.D., *Historical Review of Air-Bearing Spacecraft Simulator*, Journal of Guidance, Control, and Dynamics, Vol.26, No.4, July-August 2003.
- [3] Gavrilovich I., Krut S., Gouttefarde M., Pierrot F., Dusseau L., *Test Bench For Nanosatellite Attitude Determination And Control System Ground Tests*, 4S Symposium 2014.
- [4] Gavrilovich I., Krut S., Gouttefarde M., Pierrot F., Dusseau L., *Robotic Test Bench For CubeSat Ground Testing: Concept and Satellite Dynamic Parameter Identification*, IEEE/RSJ International Conference on Intelligent Robots and Systems, pp. 5447-5453, 2015.
- [5] New Way Air bearings <http://www.newwayairbearings.com/design/detailed-product-information>
- [6] Simone C., et al., *A Dynamics, Hardware-in-the-Loop, Three-Axis Simulator of Spacecraft Attitude Maneuvering with Nanosatellite Dimensions*, JoSS, Vol. 4, No. 1, pp. 315-328, 2015.

- [7] Prado J., et al., *Three-Axis Air-Bearing Based Platform For Small Satellite Attitude Determination and Control Simulation*, Journal of Applied Research and Technology, Vol. 3, No. 3, December 2005.
- [8] C. W. Crowell, *Development and analysis of a small satellite attitude determination and control system testbed*, Massachusetts, 2011.
- [9] B. N. Agrawal and R. E. Rasmussen, *Air bearing based satellite attitude dynamics simulator for control software research and development*, Proc.SPIE, Technologies for Synthetic Environments: Hardware-in-the-Loop Testing, vol. 4366, pp. 204-214, 2001.
- [10] M. A. Peck and A. R. Cavender, *An airbearing-based testbed for momentum-control systems and spacecraft line of sight*, Advances in the Astronautical Sciences (American Astronautical Society), pp. 427-446, 2003.
- [11] Boynton R., *Using A Spherical Air Bearing To Simulate Weightlessness*, 55th Annual Conference of the Society of Allied Weight Engineers, June 1996.